

Numerical modeling and scaling of high heat flux subcooled boiling heat transfer

ANTHONY CASTROGIOVANNI

GASL Inc., 77 Raynor Ave., Ronkonkoma, NY 11779, U.S.A.

and

PASQUALE M. SFORZA

Polytechnic University, 6 Metrotech Center, Brooklyn, NY 11201, U.S.A.

(Received 22 June 1993 and in final form 22 October 1993)

Abstract—The development of a numerical model for analyzing and scaling boiling phenomena in a circular cooling passage subjected to high heat flux is described. The model is used to solve the conjugate conduction/convection heat transfer problem for a variety of fluid and geometric parameters. The results provide detailed information, describing the essential features of the heat transfer process. This, along with recent observations of high heat flux boiling phenomena, is used to formulate a reasonable analytic scaling law. A glass–refrigerant system is then analyzed as a potential model for a copper–water system, facilitating laboratory-scale study.

INTRODUCTION

EXTREMELY high heat flux operation poses a challenge for many industries. Heat fluxes exceeding 45 MW m^{-2} ($4000 \text{ BTU ft}^{-2} \text{ s}^{-1}$), for example, are experienced at the throat of a wind tunnel nozzle during true enthalpy simulation of hypersonic flight. Cooling system design suffers from over-conservatism arising from the lack of detailed analytical information. Phase change heat transfer, for example, is often avoided due to the scarcity of ‘design oriented’ engineering relations and fear of critical heat flux (CHF). The simple, commonly used cooling channel configuration shown in Figs. 1(a) and (b) can benefit from permitting nucleate boiling heat transfer to occur. This cooling channel configuration offers significant advantages over shell-in-tube types due to the inherent mechanical continuity between the heated surface and the cooler outer structure. A closed form solution for this configuration is not available. For simplicity, this practical configuration is idealized to the unit problem shown in Fig. 1(b). A periodic distribution of cooling holes located a given distance from a heated surface can be broken up by assuming that each cooling passage has a unique ‘zone of influence’ beyond which it has no effect.

The case of a circular hole in a semi-infinite medium is often referred to as the ‘pipe buried in the ground’ problem. The boundary conditions considered in much of the existing literature, however, are limited to ideal situations which rarely occur in practice. The most common of these is the assumption that the surface of the circular cooling passage and the heated

surface are both held at constant temperature. In the actual case, the temperatures along these surfaces vary, as do the convective heat transfer coefficients. Existing approximate methods which incorporate convective boundary conditions ultimately lead to results which are still limited in application.

In an effort to reduce the number of assumptions required to analyze this heat transfer problem, a parametric nonlinear finite element analysis is selected to study it numerically. Convective heat transfer coefficients which are dependent on wall temperature are modeled as such, thus more appropriately simulating the nonlinearity of the practical case. Additionally, traditional conservative nucleate boiling heat transfer relations are used in the formulation of water film coefficients to examine the effects of local boiling on the portion of the cooling passage closest to the heated surface. These results show an appreciable improvement in the cooling capability over that of the identical arrangement without boiling, while temperatures remain safely below the CHF value.

Experimental studies of boiling heat transfer in the range of heat fluxes pertinent to rocket nozzles and other high energy systems are costly and dangerous so the ability to model the problem with a benign experimental apparatus is of particular interest to designers. To provide an economical, meaningful experiment requires the ability to scale the physical processes occurring. The scaling of two phase flow heat transfer has received some attention in the past, e.g. refs. [1, 2], which resulted in the introduction of various non-dimensional quantities. The available literature emphasizes thermodynamic scaling of the

NOMENCLATURE

A	area	Greek symbols	
C_p	specific heat at constant pressure	θ	polar angle, see Fig. 2
d	diameter	μ	viscosity
F	geometric scale factor	ρ	density
H	hole spacing	σ	surface tension of liquid-vapor interface.
h_{fi}	convective heat transfer or film coefficient		
h_{fg}	enthalpy of vaporization at saturation temperature	Subscripts	
k	thermal conductivity	approx.	approximate
L	distance along cooling passage	avg	average
l	distance of hole centerline from heated surface	b	boiling
m	mass	bulk	evaluated at bulk conditions
P	pressure	d	based on diameter
Q	heat	FC	forced convection
\dot{Q}	heat flow	fi	evaluated at film conditions
q	heat flux	g	saturated vapor conditions
r	radius	h	hydraulic
R	thermal resistance, $\Delta T/\dot{Q}$	ib	incipient boiling
t	thickness	l	liquid
t	time (equation (1))	K	from Kutateladze [11]
T	temperature	p	evaluated at constant pressure
ΔT_{sat}	$T_{wall} - T_{sat}$	sat	at saturation temperature
V	velocity	sb	subcooled boiling
x, y, z	Cartesian coordinates.	v	vapor
		w	wall
		wall	at wall.

fluid so as to reduce the required heat input necessary to induce boiling. It is also generally presumed that any geometric scaling would invalidate similarity because bubble size is independent of passage size. The current work is aimed at providing a complete scaling of the practical heat transfer problem of Fig. 1 combining fluid, geometry, and heat transfer as the basis for the design of a simple and versatile laboratory-scale experimental apparatus.

NUMERICAL ANALYSIS

A finite element model (FEM) was generated using EMRC NISA II software on a 386-20 personal computer (see Fig. 2). The parametric study described subsequently was performed by analyzing various combinations of hole spacing (or model width), distance of the hole from the heated surface, input heat flux, and cooling flow conditions.

Material properties used were those of oxygen free, high conductivity (OFHC) copper. Three surfaces of the rectangular region are adiabatic boundaries while the fourth and the hole surface are convective. For the purpose of the parametric study, the ambient temperature of the hot gas is fixed at 1667 K (3000°R), while the ambient temperature of the water, $T_{bulk, water}$, is held at 300 K (540°R). Three-dimensional effects in the real case would arise from the variation of $T_{bulk, water}$ along the cooling passage length.

The governing equation of heat transfer used by the finite element code is a two-dimensional form of Fourier's law of heat conduction,

$$\frac{\partial}{\partial x} \left(k_x \frac{\partial T}{\partial x} \right) + \frac{\partial}{\partial y} \left(k_y \frac{\partial T}{\partial y} \right) = \rho C_p \frac{\partial T}{\partial t} \quad (1)$$

and is applicable for a length of cooling passage (L) corresponding to an acceptably small value of $\Delta T_{bulk, water}$ as given by the relation

$$L = \frac{\rho V \frac{\pi d^2}{4} C_p \Delta T_{bulk, water}}{\dot{q} H} \quad (2)$$

where H is the hole spacing. The convective boundary conditions can be expressed by Newton's law of cooling, $\dot{q} = h_h(T_{wall} - T_{fluid})$. On the heated surface the hot gas film coefficient is held constant whereas on the cooling passage surface the water film coefficient is considered to be a function of wall temperature. The circumferential variation of film coefficient around the cooling passage can be very large, particularly in cases in which the cooling water boils locally in the region of the cooling hole closest to the heated surface. The FEM reads these temperature dependent film coefficients from a data table of h_h vs T generated using relations described in the next section. This dependency of h_h on wall temperature necessitates the use of a nonlinear solution scheme which implements

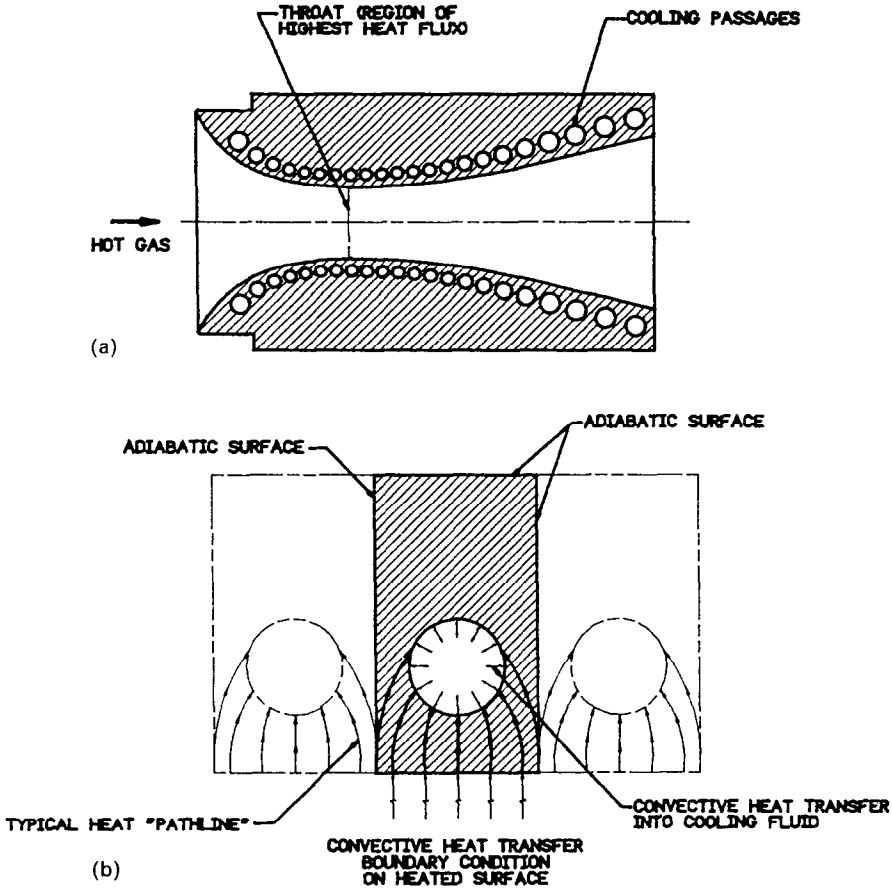


FIG. 1. (a) Typical heat exchanger. (b) Unit problem configuration.

full Newton–Raphson iteration. A tolerance of 0.001 is used for the heat flux to control the accuracy of the converged solution. If the solution does not converge, the code reformulates its solution matrix to update the temperature dependent boundary condition. For

transient analysis, the input time step is reduced automatically until convergence is achieved.

CORRELATIONS FOR FORCED CONVECTION WITH BOILING

In cases where the fluid bulk temperature is maintained below saturation, i.e. forced convection with subcooled boiling, the heat flux can be calculated by the following relation from Holman [3]:

$$\dot{q}_{sb} = \dot{q}_{FC} + \dot{q}_b \tag{3}$$

The component of heat flux due to forced convection (\dot{q}_{FC}) is found using the Dittus–Boelter equation [4]

$$\dot{q}_{FC} = 0.023 \frac{k}{d} Re_d^{0.8} Pr^{0.3} (T_{wall} - T_{bulk, water}) \tag{4}$$

Here the Reynolds number, Prandtl number and thermal conductivity are all evaluated at the film temperature

$$T_{fi} = \frac{T_{wall} + T_{bulk, water}}{2} \tag{5}$$

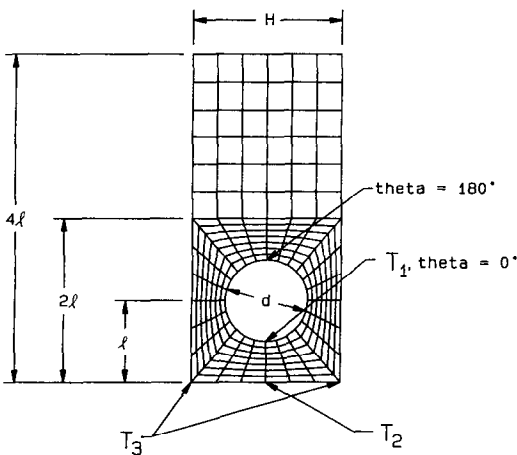


FIG. 2. Finite element mesh.

The contribution due to boiling \dot{q}_b is found using the correlation proposed by Rohsenow [5]

$$\dot{q}_b = \left[\frac{C_{p,l} \Delta T_{sat}}{0.013 h_{fg} Pr} \right]^3 \mu_l h_{fg} \left[\frac{(\rho_l - \rho_v)}{\sigma} \right]^{1/2} \quad (6)$$

where $\Delta T_{sat} = T_{wall} - T_{sat}$. The applicability of equation (6) is limited by the fact that the incipience of boiling does not necessarily coincide with the point at which $T_{wall} = T_{sat}$. The heat flux at which a liquid begins to boil is a function of surface finish, bubble structure, and thermal boundary layer, among other things. The relationship defining incipient boiling used here is taken from Davis and Anderson [6]:

$$\dot{q}_{ib} = \frac{k_l h_{fg} \rho_v}{8 C_b \sigma T_{sat}} \quad (7)$$

The constant C_b may be 1 for hemispherical or 2 for spherical bubble nuclei. Since experimental results show data falling between these values, and $C_b = 2$ yields lower \dot{q}_{ib} values, this more conservative value is selected. It is important to note that various studies [7] have shown that correlations for h_{fg} can vary significantly depending on flow conditions.

Uncertainty in forced convection boiling lies mainly in the prediction of the CHF point. No single correlation to date is capable of accurately predicting CHF over a wide range of parameters. Despite the scarcity of detailed information pertaining to CHF, careful interpretation of references such as Schaefer and Jack [8], Jens and Lottes [9], and Remizov and Sapankerich [10] can allow for conservative assumptions of its magnitude. Over the range of heat fluxes and water flow rates pertinent to this paper, CHF is not expected to occur at $\Delta T_{sat} < 55.6$ K (100°R). In order to remain safely below this region, an upper limit of $\Delta T_{sat} = 27.8$ K (50°R) has been incorporated into the numerical analysis.

Equations (3)–(7) were used to calculate tables of film coefficient vs wall temperature for 4.14 MPa (600 psia) water at bulk velocities of 12.2, 18.3 and 24.4 m s⁻¹ (40, 60 and 80 ft s⁻¹), where the bulk temperature of the water is held constant at 300 K (540°R). Three different tables were generated for each velocity. The first does not take boiling into account and hence uses equation (5) exclusively. For given values of flow rate, and wall and film temperatures incipient boiling occurs when the calculated forced convection heat flux is equal to the incipient boiling value at the given wall temperature. For cases in which boiling is considered, a computer program was written to iteratively solve for the T_{wall} that satisfies one of the following:

$$\dot{q}_{ib} = \dot{q}_{FC}$$

or

$$\frac{k_l \lambda \rho_v}{8 C_b \sigma T_{sat}} = 0.023 \frac{k}{d} Re_d^{0.8} Pr^{0.3} (T_{wall} - T_{bulk, water}). \quad (8)$$

At this T_{wall} , the effect of boiling is introduced into the film coefficient formula using equations (3)–(7). The second of the three tables includes boiling effects, but limits the wall temperature to approximately 13.9 K (25°R) above saturation. Since the boiling film coefficient is proportional to ΔT_{sat}^3 , a relatively small temperature rise above saturation such as this can increase the heat transfer rate considerably. Cases run with this table are labeled as incipient boiling. The third table limits T_{wall} to the point at which $\Delta T_{sat} = 27.88$ K (50°R). This condition is referred to as moderate boiling.

RESULTS OF PARAMETRIC STUDY

Nine geometric models were used to study the effects of variations in the distance of the hole from the heated surface and in hole spacing. For each model, steady state runs which required between five to ten minutes of processing time each, were performed on a trial and error basis to determine the hot gas film coefficients which induce the three levels of boiling described previously. Transient runs required six to eight hours per run to achieve a convergent steady solution. A grid study, which was not performed, would have most likely resulted in a refinement of the mesh in the critical regions of the FEM.

Some model verification solutions using isothermal boundary constraints were obtained and compared to closed form solutions found in Kutateladze [11] which is based on a source/sink representation of the temperature field. Nodal temperatures from the numerical solution were found to agree within 0.5% of the analytically predicted values. Constant film coefficient boundary conditions were also used to compare with results using the approximate method described by Kutateladze. Results of the approximate method for high heat flux boundary conditions were as much as 20% more conservative than those obtained numerically, i.e. the approximate method resulted in lower heat removal capability than the equivalent case examined numerically.

The effect of boiling can be appreciated by comparing the heat flow (\dot{Q}) values from the Table 1. Increased heat removal capability on the order of 15–25% can be achieved by inducing subcooled boiling, while remaining substantially below the expected CHF point. These results, coupled with the efficiency of the solution for the conduction problem, can be of vital significance to the heat exchanger designer or analyst faced with the limitations of single phase water cooling.

APPROXIMATE METHOD

One of the goals of the research described in this paper is to provide a design/analysis tool to calculate the heat removal capability of the circular cooling passage *without* having to carry out a detailed numerical analysis. To accomplish this, the following tech-

Table 1. Heat flow comparisons

Model no.	Hole depth [cm (in)]	Hole spacing [cm (in)]	\dot{Q} No boil [W (BTU s ⁻¹)]	\dot{Q} Incip. boil [W (BTU s ⁻¹)]	\dot{Q} Mod. boil [W (BTU s ⁻¹)]
1	0.546 (0.215)	1.14 (0.45)	7206 (6.83)	7808 (7.40)	8356 (7.92)
2	0.635 (0.250)	1.14 (0.45)	7163 (6.79)	7786 (7.38)	8272 (7.84)
3	0.953 (0.375)	1.14 (0.45)	7101 (6.73)	7808 (7.40)	8156 (7.73)
4	0.546 (0.215)	1.40 (0.55)	8145 (7.72)	8789 (8.33)	9421 (8.93)
5	0.635 (0.250)	1.40 (0.55)	7976 (7.56)	8609 (8.16)	9210 (8.73)
6	0.953 (0.375)	1.40 (0.55)	7913 (7.50)	8616 (8.20)	9169 (8.69)
7	0.546 (0.215)	1.65 (0.65)	8958 (8.49)	9611 (9.11)	10 245 (9.71)
8	0.635 (0.250)	1.65 (0.65)	8799 (8.34)	9390 (8.90)	10 034 (9.51)
9	0.953 (0.375)	1.65 (0.65)	8599 (8.15)	9380 (8.89)	10 002 (9.48)

nique is proposed to calculate an equivalent water film coefficient to use in the equation for thermal resistance found in Kutateladze [11]. This resistance equation may be written as

$$R_k = \frac{1}{2\pi L} \left[\frac{1}{h_k r} + \frac{1}{k} \ln \left(\frac{1}{\pi r} \sinh \left(2\pi \frac{l+k/h_{fi, gas}}{H} \right) \right) \right] \quad (9)$$

where h_k a constant film coefficient on the cooling passage surface. This equation is derived by modifying the solution of the conduction problem for isothermal boundaries (source/sink solution) using the 'additional wall method' described in detail in ref. [11].

From the numerical data generated, an overall heat flow quantity for the area of interest is found using the relation

$$\dot{Q} = h_{gas} L H \left(T_{gas} - \frac{T_2 + T_3}{2} \right) \quad (10)$$

and a thermal resistance is defined by

$$R_N = \frac{T_{gas} - T_{bulk, water}}{\dot{Q}} \quad (11)$$

Then setting R_N equal to R_k permits the calculation of the equivalent constant water film coefficient h_k . However, one requires some other means to determine h_k when no numerical result is available.

Given the task of analyzing the heat transfer in a practical device such as that shown in Fig. 1, the geometry first must be reduced to the unit problem of Fig. 2. The length of the cooling passage must be divided into a number of regions which satisfy equation (2), and the hole spacing should be such that a quasi-isothermal heated surface may be expected. A hole spacing (H) equal to the hole diameter (d) plus the material thickness (t) is a good rule of thumb

value. The film coefficient of heat input from the hot gas must be known and a value of ΔT_{sat} must be chosen to induce the desired degree of boiling, if any. The following relation from Trucco [12] can be used to determine the distance of the hole centerline from the heated surface which produces an acceptable hot surface temperature:

$$\frac{k}{l-d} (T_{sat} + \Delta T_{sat} - T_{hot wall}) = h_{gas} (T_{gas} - T_{hot wall}) \quad (12)$$

An average wall temperature for the cooling surface may be found from

$$T_{wall, avg} = \frac{T_{sat} + \Delta T_{sat} + T_{bulk, water}}{2} \quad (13)$$

and an approximate water film temperature may be given by

$$T_{fi, avg} = \frac{T_{wall, avg} + T_{bulk, water}}{2} \quad (14)$$

Finally, an approximate water film coefficient may be calculated using the Dittus-Boelter equation with properties evaluated at $T_{fi, avg}$ as follows:

$$h_{approx.} = 0.023 \frac{k}{d} Re_d^{0.8} Pr^{0.3} \quad (15)$$

A comparison of the film coefficients h_k and $h_{approx.}$ calculated by the above method yields the following relationship (see Fig. 3):

$$h_k = 0.0462 + 1.44 \times 10^{-4} h_{approx.} V^{3.151} \quad (16)$$

Hence, the equivalent film coefficient calculated in this fashion may be used in equation (10) to determine a more realistic thermal resistance. Note that, in equation (17), the units of h_k and $h_{approx.}$ are [MW m⁻² s⁻¹ K⁻¹] and the units of velocity are [m s⁻¹]. This thermal

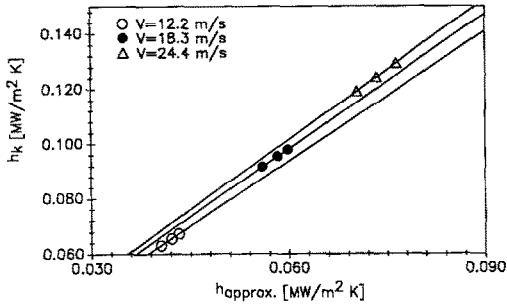


FIG. 3. Correlation of h_K vs $h_{\text{approx.}}$.

resistance, in combination with the difference in bulk temperatures of the hot and cold fluid, can now be used to calculate a characteristic heat flow. It is important to emphasize that this equation is derived for the range of parameters pertinent to this paper and its application is thus limited. This approximation has been applied to the 81 cases studied herein and 95% of the results are within 4% of those achieved by numerical analysis (the remaining 5% are within 8%).

SCALING

Many scaling and modeling parameters for the study of single phase fluid flow have been developed over the years to predict similarity between flow systems. It is important to note that, although the traditional dimensionless groups used for this purpose are generally agreed upon, it is difficult to achieve more than partial simulation in practice.

References [1, 2] outline a number of quantities derived from non-dimensionalizing the characteristic equations for one-dimensional two phase flow. Various simplifying assumptions are required in order to reduce the inherent complexity associated with the covariance between parameters such as enthalpy and pressure, etc. It becomes apparent that, for the complexity of the configuration in Figs. 1 and 2, the application of analytical scaling techniques to this practical problem is a considerable, if not insurmountable challenge.

Intuition suggests that identification of 'modeling fluids' which require less heat input to induce boiling, yet possess characteristics similar to the actual fluid, would be a necessary component in a scaling exercise. Another issue of importance in scaling is the possibility of replacing the usual conduction medium (like copper) with one which couples both appropriate thermal properties and optical transparency for visualization purposes and so that non-intrusive diagnostics may be implemented. The derived benefits of scale modeling of high heat flux boiling apparatus are enormous when one considers the cost and safety issues involved. The nuclear reactor and rocket engine industries for example would benefit from reducing both the heat input and the geometric size of their models while the microelectronics industry may desire a model which scales up their configurations of inter-

est. In any case, a laboratory scale apparatus can provide a wealth of both design and scientific information otherwise unavailable.

Figures 4 and 5 depict typical thermal contours for copper/water and glass/Freon boiling heat transfer systems, respectively. The likeness between the profiles as well as their apparent 'flatness' suggests that a one-dimensional simplification of the conduction problem is possible for appropriate (and practical) hole spacing. Typical azimuthal temperature profiles around a cooling passage follow a sinusoidal curve with the highest value on the passage surface closest to the heated surface. This suggests that the problem may be reduced to one of calculating the appropriate coolant boundary condition, calculating a coolant-side surface temperature, and performing a 1-D conduction analysis for the centerline ($\theta = 0$) of the cooling passage. In the steady case, the pertinent properties of the solid material would then be the thermal conductivity and the thickness t (see Fig. 2) making the scaling of the conduction medium fairly straightforward.

The fluid parameters of importance are the velocity, entering temperature, liquid and vapor phase densities, enthalpy of vaporization, viscosity, specific heat, thermal conductivity, and surface tension. It is here that one finds difficulty in ensuring similarity between scaling fluids.

The extreme heat flux conditions of interest require flows characterized by a high degree of subcooling and bubbles which are very small in comparison to passage size. Such flows are characterized by high velocities, or, more accurately, large values of friction velocity

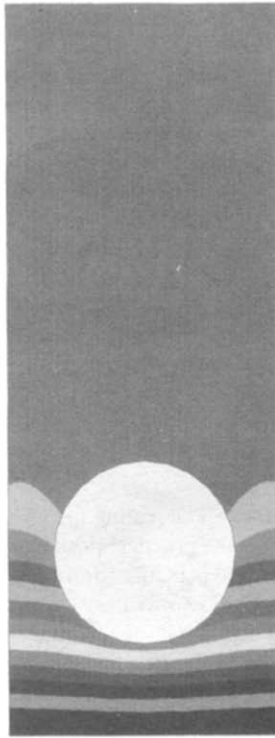
$$u_* = \sqrt{\left(\frac{\tau_w}{\rho_l}\right)} \quad (17)$$

where τ_w is the wall shear. Vandervort *et al.* [13] found that, for a heat flux of 30 MW m^{-2} , a subcooling of 373 K, a water mass flux of $25000 \text{ kg m}^{-2} \text{ s}^{-1}$, and a tube diameter of 1.07 mm, the bubble diameters are on the order of $3 \mu\text{m}$. This number is in agreement with that obtained using Levy's bubble departure diameter [14] which accounts for all forces which act on the bubble.

Bubble diameters this small tend to reinforce the notion that the boiling behavior is not sensitive to passage size (within reasonable limits). Similarly, high subcooling ($T_{\text{bulk, fluid}} - T_{\text{sat.}}$) results in a bubble layer no more than a couple of bubble diameters thick [13]. This small bubble layer diminishes the extent to which boiling affects the dynamic behavior of the flow in terms of pressure drop, etc..

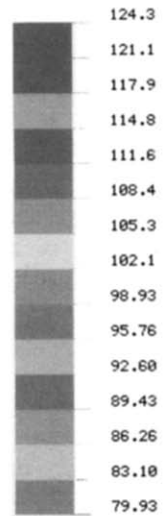
The most important parameters in Fig. 2 from a design point of view are the absolute temperatures on the heated surface and the differential temperature between the heated surface and the cooling passage surface. This of course assumes that the fluid is well below the critical heat flux (CHF). To simplify the

EMRC - DISPLAY II POST-PROCESSOR VER 91.0 Dec/ 2/93



ISOTHERM CONTOUR
STEADY-STATE HET
VIEW : 7.99E+02
RANGE: 1.24E+03

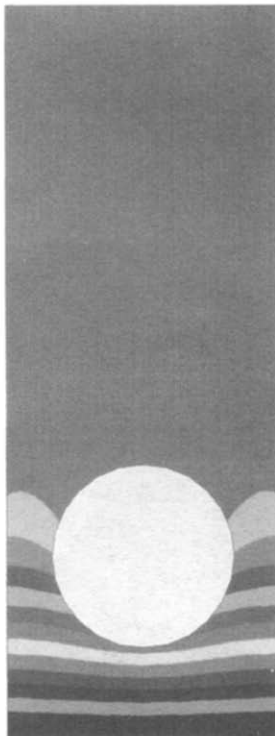
(Band x 1.0E1)



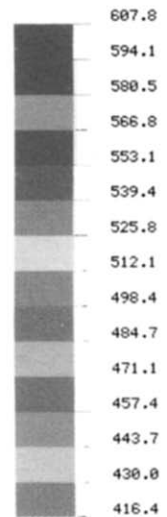
Y RX= 0
Z X RY= 0
RZ= 0

FIG. 4. Copper/water cooling system configuration.

EMRC - DISPLAY II POST-PROCESSOR VER 91.0 Dec/ 2/93



ISOTHERM CONTOUR
STEADY-STATE HET
VIEW : 4.16E+02
RANGE: 6.08E+02



Y RX= 0
Z X RY= 0
RZ= 0

FIG. 5. BK-7/Freon-12 cooling system configuration.

analysis for scaling we therefore limit our attention to the line $\theta = 0$ of the cooling passage. It is found from the data of the parametric study that along this centerline the following energy balance equation holds true:

$$\frac{k(T_{\text{hot}} - T_{\text{hole}})}{t} = h_{\text{fi}}(T_{\text{hole}} - T_{\text{bulk,fluid}}) \quad (18)$$

where h_{fi} , also a strong function of T_{hole} , is found by equations (4) and (5) and T_{hot} is the temperature of the heated surface. Rearranging this one-dimensional equation yields a Biot number for the system, defined as

$$Bi = \frac{h_{\text{fi}} t}{k} = \frac{(T_{\text{hot}} - T_{\text{hole}})}{(T_{\text{hole}} - T_{\text{bulk,fluid}})} \quad (19)$$

which is the fundamental similarity parameter for our problem. For proper scaling it is necessary to keep the system Biot number in the laboratory experiment equal to that in the real device.

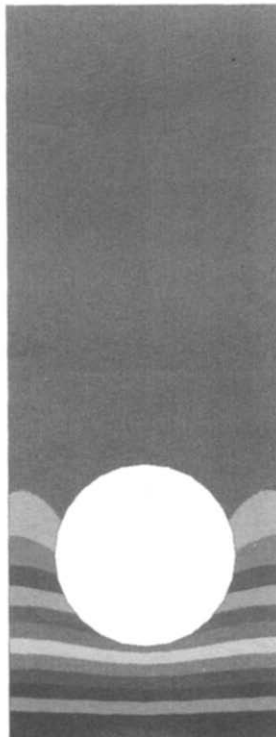
In designing a scaled experiment one chooses a fluid, for example Freon, which changes phase at a low temperature and then calculates a film coefficient keeping ΔT_{sat} the same as in the real device. A reasonable subcooling is selected and the right hand side of equation (18) is used to calculate a heat flux. The material for the conduction medium, glass for example, is then chosen and the thickness t is deter-

mined as that which keeps the system Biot number constant. The combination of material and thickness may not yield an acceptable T_{hot} in which case either another material or another fluid must be chosen. At this point an experiment has been designed which approximately scales the real system. Variation of the heat flux in the real device will yield a change in field temperatures. By maintaining the Biot number constant between systems, temperature differences measured in the laboratory experiment (with modified heat flux) should always be directly scalable to those in the original system. The problem now reduces to one of finding practical material/fluid combinations which are compatible with this scaling theory.

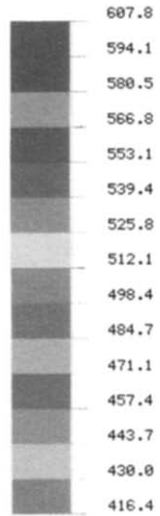
RESULTS OF SCALING

The scaling theory described above was applied to the practical problem of cooling passages typical of a hypersonic wind tunnel nozzle throat similar to that shown in Fig. 1(a). Choosing OFHC copper as the conduction medium and values of heat flux and water flow rate appropriate to subcooled boiling, a system Biot number of 0.52 is obtained. Selecting Freon as the scaling fluid and adjusting the fluid velocity to obtain a film coefficient vs ΔT_{sat} curve similar to the water case, the film coefficient required to induce the

EMRC - DISPLAY II POST-PROCESSOR UER 91.0 Dec/ 2/93



ISOTHERM CONTOUR
STEADY-STATE HET
VIEW : 4.16E+02
RANGE: 6.08E+02



Y RX= 0
Z RY= 0
X RZ= 0

FIG. 6. Nickel/Freon-12 cooling system configuration.

same degree of boiling is found to be approximately one-seventh the water value or

$$h_{fi, \text{Freon}} = \frac{h_{fi, \text{water}}}{7}. \quad (20)$$

Similarity between the film coefficient curves can be established through non-dimensionalizing $h_{fi}(\Delta T_{\text{sat}})$ by dividing by $h_{fi}(\Delta T_{\text{sat}} = 0)$. BK-7 glass is chosen because of its high thermal conductivity (relative to other transparent materials) given by

$$k_{\text{BK-7}} = \frac{k_{\text{copper}}}{32.51} \quad (21)$$

and high useful operating temperature (860 K continuous). We find that using F as a geometric scale factor and equating system Biot numbers yields

$$F = \frac{1}{4.64}. \quad (22)$$

Thus the glass/Freon model must be approximately 20% as large and will operate at sixteen times less heat flux as the real device. Similarly it is found that a nickel/Freon model will be roughly double the size of the real device. Although such a system does not offer optical transparency, a large nickel model would facilitate the use of conventional fabrication and instrumentation techniques. Figures 4–6 depict copper/water, BK-7/Freon-12 and nickel/Freon-12 systems which possess the same Biot number. Comparing temperature differences between corresponding points in the geometrically similar models reveals that the temperature differences in the copper/water model are 2.318 times greater than those in either the BK-7/Freon or the nickel/Freon models, which have identical thermal profiles. This temperature difference scaling factor is equal to the ratio of $T_{\text{hot}} - T_{\text{bulk, fluid}}$ from the copper/water system to $T_{\text{hot}} - T_{\text{bulk, fluid}}$ from the BK-7/Freon or nickel/Freon systems. These results reinforce the scaling theory described. Further research is planned to experimentally verify the scaling procedure outlined above and to identify additional practical material/fluid combinations appropriate to experimental study.

CONCLUSIONS

A parametric numerical study of a circular water cooling hole in a semi-infinite rectangular region subject to large convective heat addition on one side has been presented. A correlation has been developed for the calculation of an equivalent water film coefficient that may be used in an existing closed form solution which would otherwise not be applicable in the range of high heat flux cooling treated here. Additionally, the effects of conservative nucleate boiling are shown

to increase the heat removal capability of a fixed geometry by as much as 25% while temperatures remain substantially below those associated with CHF. A technique for developing scaling relationships for circular cooling passages subject to high heat flux and nucleate boiling is also described. Reduction of required heat input and hardware temperatures are the motivation for developing a benign experimental apparatus to investigate the characteristics of such devices. The Biot number of the passage centerline is identified as the important similarity parameter for flow systems which are characterized by high subcooling and high friction velocity, and therefore thin bubble layers. Results of the application of this scaling theory to a practical copper/water system indicate that glass/Freon and nickel/Freon models which operate at a fraction of the heat flux in the real device are viable simulants.

REFERENCES

1. F. Mayinger, Scaling and modelling laws in two phase flow and boiling heat transfer. In *Two Phase Flow and Heat Transfer in the Power and Process Industries* (Edited by A. E. Bergles *et al.*). Hemisphere, New York (1981).
2. M. Ishii and O. C. Jones, Jr., Derivation and application of scaling criteria for two phase flows. In *Two-Phase Flows and Heat Transfer* (Edited by S. Kakac and T. N. Veziroglu), Vol. 1, pp. 163–186. Hemisphere, New York (1977).
3. J. P. Holman, *Heat Transfer* (6th Edn), p. 510. McGraw-Hill, New York (1986).
4. W. H. McAdams, *Heat Transmission* (2nd Edn), p. 183. McGraw-Hill, New York (1942).
5. W. M. Rohsenow, Boiling. In *Handbook of Heat Transfer* (Edited by W. M. Rohsenow and J. P. Hartnett), Chap. 13. McGraw-Hill, New York (1973).
6. E. J. Davis and G. H. Anderson, The incipience of nucleate boiling in forced convection flow, *A.I.Ch.E. J.* **12**, 774–780 (1966).
7. V. P. Carey, *Liquid-Vapor Phase Change Phenomena*, Chap. 12, Fig. 12.17. Hemisphere, New York (1992).
8. J. W. Schaefer and J. R. Jack, Investigation of forced convection nucleate boiling of water for nozzle cooling at very high heat fluxes, NASA TN D-1214 (1962).
9. W. H. Jens and P. A. Lottes, Analysis of heat transfer, burnout, pressure drop and density data for high pressure water, ANL-4627, Argonne National Laboratory (1951).
10. O. V. Remizov and A. P. Sapanerich, Burnout with non-uniform distribution of heat flux over the perimeter of a round tube, *Teploenergetica* (in Russian) (1975).
11. S. S. Kutateladze, *Fundamentals of Heat Transfer*, pp. 89–99. Academic Press, New York (1963).
12. H. A. Trucco, Design of a 2D water cooled nozzle for the NASA LaRC ceramic heated tunnel, GASL TR under NASA contract NAS1-15358 (1979).
13. C. L. Vandervort, A. E. Bergles and M. K. Jensen, Heat transfer mechanisms in very high heat flux subcooled boiling, ASME Winter Annual Meeting, Symposium on High Heat Flux Accommodation, Anaheim CA, Nov. (1992).
14. J. G. Collier, *Convective Boiling and Condensation* (2nd Edn), p. 181. McGraw-Hill, U.K. (1981).